SIViP (2014) 8:765–778
DOI 10.1007/s11760-013-0582-7

ORIGINAL PAPER

Multi-resolution Fourier analysis: time-frequency resolution in excess of Gabor–Heisenberg limit

Nourédine Yahya Bey

Received: 22 May 2013 / Revised: 5 September 2013 / Accepted: 18 November 2013 / Published online: 3 December 2013

Abstract In this paper, multi-resolution Fourier analysis, labeled NY-MFA, suitable for time-varying spectra is proposed. It is shown that increasing time resolution has no detrimental effects on frequency resolution and achieved resolution bounds are in excess of Gabor–Heisenberg limit. Observation results with their increased time resolution, discriminated and precise frequency contents justify thoroughly the assumption of stationarity and consequently approach more precisely the concept of frequency and its changes than wavelets and short-term Fourier transform can do.

Keywords Time-frequency analysis · Time-frequency trade-off · Short-term Fourier transform · Gabor–Heisenberg inequality · Time-varying spectra · Frequency estimation · Stationarity · Doppler signal

1 Introduction

Time-frequency analysis with its interdisciplinary origins represents an important field of modern harmonic analysis and applications [1]. Mapping a one-dimensional signal into a two-dimensional function of time and frequency or scale is a wide spread tool for the analysis of non-stationary signals that arise in many real-world situations. One of the important and widely used time-frequency analysis is based on the Fourier transform. Note that no attempt is made here in the proposed reference section to summarize innumerable applications of short-term Fourier transform (STFT) in various areas of science and industry (radar and sonar data processing, geophysical and seismic exploration, biomedical engineering, non-destructive testing, and so on [2–11]). STFT determines the sinusoidal frequency and phase contents of local sections of a signal as it changes over time. The signal to be transformed is multiplied by a window function which is defined to be nonzero over only a short period of time. Fourier transform is taken as the window slides along the time axis. Resulting transform is a two-dimensional time-frequency representation of the signal. One of well-known drawbacks of STFT is its fixed resolution. The width of the windowing function defines frequency resolution (or how close spectral components can be separated) or good time resolution (instants at which frequencies change). A unavoidable trade-off arises between the length of time interval T and frequency width ΔB so that $T\,\Delta B = 1$, whereas the theoretical limit is given by Gabor–Heisenberg inequality [12]. Increasing frequency resolution causes a larger window size and therefore deteriorating time resolution and vice-versa.

In order to overcome shortcomings of STFT or its square modulus called spectrogram (quadratic time-frequency representations), one finds also other non-stationary signal representations known to have better resolution as the Cohen's class and bilinear time-frequency energy distributions [13–15]. Among these distributions, much attention was drawn to the bilinear Wigner–Ville distribution in spite of its non-linearity. Its use shows the presence of non-negligible cross-terms that result from interactions between signal components. Other methods based on the concept of scale (wavelet transform) rather than frequency are also proposed [16,17]. As pointed out in [18], the major drawback of these large variety of existing methods is their inability to propose good concentration of signal components with no misleading interference terms. This characteristic is termed readability since it is necessary for easy visual interpretation of outcomes of these representations. Improving readability of such methods

N. Yahya Bey (✉)
Faculté des Sciences et Techniques, Université François Rabelais, Parc de Grandmont, 37200 Tours , France
e-mail: nouredine.yahyabey@phys.univ-tours.fr

(bilinear time-frequency and timescale representations) aims to improve sharpness of localization of signal components [18]. If this reassignment method provides a higher concentration in the time-frequency plane, it depends on the signal, the used representation and does not eliminate cross-terms [18].

An alternative approach for resolution of mentioned problems is developed by wavelets [19–23]. Here also our reference section is not exhaustive, and no attempt is made to summarize innumerable applications of wavelets. In spite of their flexible resolution properties, wavelets trails drawbacks since they act as local magnifiers independently of the nature of the signal under analysis (stationary, quasi-stationary or not) and necessitate skillful selection of appropriate wavelets. Moreover, due to their complexity, interpretation of spectra is quite difficult and information on frequency is only approximative since a wavelet does not have a pure frequency as a sine wave. Characterization of a precise frequency content is therefore not suitable by means of wavelets.

In previous works [24–26], a theory called "*multi-resolution Fourier analysis*" is proposed. This theory is relabeled "*NY-MFA*" [26] in order to differentiate it from multi-resolution Fourier transform (MFT). Let us recall here also that NY-MFA is different in its fundamental conception and results from MFT [27–29]. MFT, a superset of STFT and wavelets, uses analysis windows dependent on a scale parameter that affects their size. A decreasing scaling parameter increases duration of the analysis window. Here NY-MFA, unlike MFT and other existing methods, achieves high time and frequency resolutions *without using windows*. How is this possible? The principal aim of NY-MFA is to overcome limitations of STFT (time-frequency tradeoff), drawbacks of wavelets (inability to provide precise frequency content) and nonlinearities (cross-terms) of above-mentioned distributions while preserving phase information. Given a stationary finite duration signal, the theory proposes construction of *overall signals* from this only observed one. The principal characteristic of these signals is their ability to reveal in the *frequency domain* resulting transforms whose main lobe widths between 3-dB levels, and therefore, resolutions vary as a function of their length. These constructed signals are called *multi-resolution signals* since their spectra display dramatically enhanced spectral sharpness as a function of the resolution level: double ($s = 2$), threefold ($s = 3$), fourfold ($s = 4$) and fivefold ($s = 5$). This possibility is termed here multi-resolution capability. Among pertinent advantages, one finds that resolution at any desired level is applied simultaneously to all points of the frequency axis, spectral leakage is contracted, frequency estimation is enhanced and efficient implementation is achieved. Moreover, inverse Fourier transformation of yielded spectra restores observed signals together with their *missing* parts. This possibility, *exclusive* to this analysis, is termed *missing signal recovery*. This signal restoration, achieved without errors, is called *natural extrapolation* [26] since no iteration algorithm is used for extrapolation. In [26], denoising properties of NY-MFA are derived. These new properties are used to extract short buried signals in noise independently of its nature, white or colored, Gaussian or not and its spectral extent.

In this work, Sect. 2 recalls principal results of NY-MFA with two appendixes A and B proposed for easy reference. NY-MFA theoretical framework for signals with time-varying spectra is described in Sects. 3 and 4. Our main focus of attention in this work is to emphasize the following advantages:

1. Frequency resolution is not degraded by decreasing lengths of analysis windows.
2. Achieved NY-MFA resolution bounds are in excess of Gabor–Heisenberg limit.
3. Increased time resolution justifies more thoroughly the assumption of stationarity attached to each local section and, consequently, approaches more precisely the concept of frequency and its changes than STFT and wavelets can do.

Clearly, requirements as linearity, invertibility (or recovering of missing parts) and together with a simple implementation are satisfied since properties of STFT remain unchanged by NY-MFA. In Sect. 5, NY-MFA is demonstrated via examples of signals including non-stationary Doppler signals widely used for various diagnoses as arterial occlusive disease or atherosclerosis [30–32]. We show in this work precise frequency or velocity tracking with decreasing lengths of analysis windows.

We show here that by comparing NY-MFA with above-mentioned time-frequency and timescale distributions, one finds that it is of simpler implementation, does not create cross-terms and needs no additional method for increasing signal concentration in the time-frequency plane nor any sort of smoothing. Moreover, NY-MFA does not destroy phase information of crucial use in image processing.

2 Fundamentals (NY-MFA)

In this section, we recall only principal results of [24–26]. All computations are clearly detailed in mentioned references together with observation results for simulated and experimental signals. However, for the sake of easy reference, one finds in appendixes A and B details supporting recalled results. Moreover, a simpler formulation of original computations [24] is proposed. It is crucial to notice that the aim of this section is to collect *pertinent* results in order to use them in Sect. 4 for construction of NY-MFA harmonic analysis of signals with time-varying spectra.

2.1 Definitions

Let $x(t)$ be a continuous time real and stationary signal defined for $-\infty < t < \infty$ and let $X(f)$ be its bandpass spectrum. Consider a finite duration signal $x_T(t)$ in the time interval $[0, T]$ "cut-out" from $x(t)$ and defined by,

$$x_T(t) = x(t)\Pi_T(t), \tag{1}$$

where $\Pi_T(t)$ is the rectangular window of length T.

Observed features of the short-term Fourier transform (STFT) are summarized for $x_T(t)$ by,

$$T\Delta B = 1, \tag{2}$$

where T and ΔB are, respectively, the length of observation interval and frequency width.

In order to overcome limitations of (2), our main effort described in above references is to use the only observed signal $x_T(t)$ for construction of overall signals able to reveal in the frequency domain resulting transforms whose main lobe widths between 3-dB levels, and therefore, resolutions vary as a function of the length of these signals. Expression of these overall signals, called *multi-resolution signals*, is given by,

$$\begin{aligned}\Re_{(s)}[x_T(t)] = \Pi_{2sT}(t) \sum_{p=0}^{1} [x_T(t - spT) \\ + (I[s/2]-1)x_T((sp+I[s/2])T-t)]\,,\end{aligned} \tag{3}$$

where $\Re_{(s)}[x_T(t)]$ represents the "s-resolution" operator applied to $x_T(t)$. The level of resolution in the frequency domain, as shown below, is defined by the lower script, s, where $s = 2, 3, 4, 5$ are, respectively, for double, threefold, quadruple and quintuple level of resolution. Here $I[s/2]$ is the integer part of $s/2$ and $\Pi_{2sT}(t)$ is the rectangular window of length $2sT$. For the sake of illustration, we recall in appendix A, derivation of the double resolution signal $\Re_{(s)}[x_T(t)]$ for $s = 2$.

2.2 Resolved amplitude spectrum

As already mentioned $\Re_{(s)}[x_T(t)]$ yields an "$s-$resolution signal" whose resulting Fourier transform is summarized by (see [24], appendix A for $s = 2$ or appendix B),

$$\begin{aligned}\mathrm{FT}[\Re_{(s)}[x_T(t)]] &= \widehat{X}(f, 1/(sT)) \\ &= X(f) \star H(f, 1/(sT)),\end{aligned} \tag{4}$$

where FT$[x]$ is the Fourier transform operator applied to x, $X(f)$ is the true bandpass spectrum of the continuous time signal $x(t)$ from which $x_T(t)$ is "cut-out." The symbol $\star$ denotes the convolution. Here $H(f, 1/(sT))$ is the transform of the *resulted window* involved in the definition of multi-resolution signals as specified by (3). The main lobe width between its 3-dB levels, and therefore, resolution is $\delta f = 1/(sT)$. See Appendix A where derivation of $H(f, 1/(sT))$ for $s = 2$ is detailed. The second argument $1/(sT)$ means that frequency locations of $\widehat{X}(f, 1/(sT))$ are separated by the mutual distance $1/(sT)$. The width δf in the frequency domain is therefore specified by,

$$\delta f = 1/(sT) = \Delta B/s, \tag{5}$$

where $s = 2, 3, 4, 5$.

The spectral width ΔB, denoting spectral spreading, as depicted by (2), is reduced by the resolution level $s = 2, 3, 4, 5$. Amplitude spectra are therefore obtained with enhanced spectral sharpness.

2.3 Signal reconstruction

For extraction of the true spectrum $X(f)$ up to the chosen resolution $1/(sT)$ and reconstruction of the signal in the time domain, we recall in appendix B that convenient filtering of $\widehat{X}(f, 1/(sT))$, as given by (4), is thresholding (hard or soft). After inverse Fourier transformation of the thresholded spectrum, the signal along with its missing parts whose length is sT ($s = 2, 3, 4, 5$) in the time domain is restored in accordance with applied frequency resolution. Computations are detailed for this purpose in [25].

3 NY-MFA scheme and lattice transform

Figure 1 summarizes NY-MFA functional scheme and its lattice transform.

3.1 Functional scheme

Features of the short-term Fourier transform (STFT) in 1(a) are given by (2). When dividing the time interval of length T into "s" local sections whose length is $\Delta\tau = T/s$ where $s = 2, 3, 4, 5$ and analyzing by means of STFT the provided sub-signal of length $\Delta\tau$, frequency spreading $s\Delta B$ results. Given the length $\Delta\tau$ of the analyzed signal, our effort is to overcome this frequency spreading by means of NY-MFA.

In 1(b), the functional scheme details how the sub-signal is handled by NY-MFA. It can be seen that the only observed sub-signal of length $\Delta\tau$ is, first, used to construct multi-resolution signals, as given by (3), whose length is $2s \times \Delta\tau$ for $s = 2, 3, 4, 5$. Secondly, Fourier transformation of multi-resolution signals is taken. As shown in Sect. 2, resulting transforms reveal main lobe widths between their 3-dB levels given by $\Delta B = 1/(s\Delta\tau)$. Frequency spreading, as shown by the STFT scheme in 1(a), is therefore eliminated. Hence, the product of the *widths* ΔB and $\Delta\tau$, respectively, in the frequency and time domains yields in 1(b),

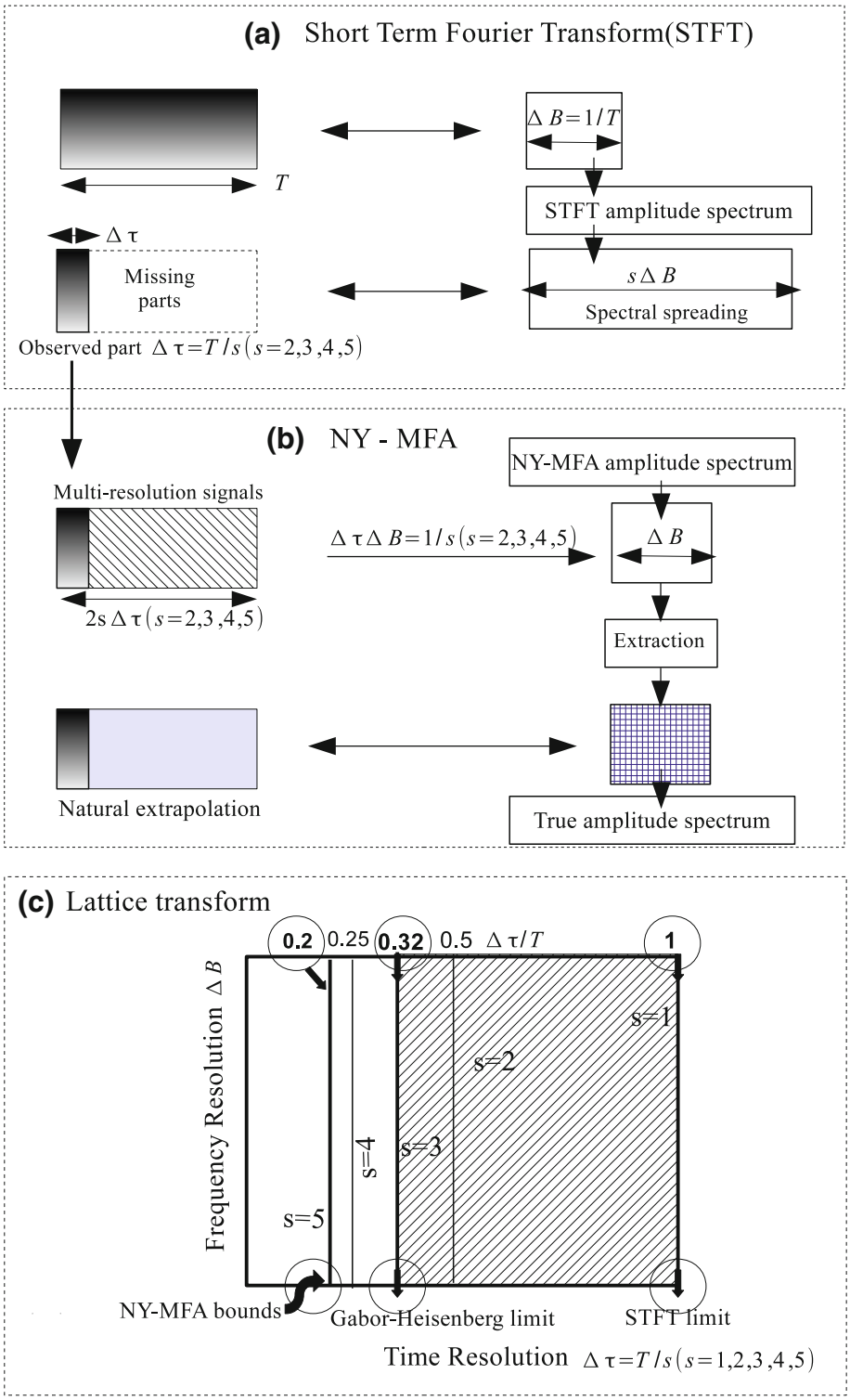

Fig. 1 Short-term Fourier transform (STFT) with its spectral spreading for decreasing time intervals is shown in **a**. NY-MFA functional scheme in **b** eliminates spectral spreading by using multi-resolution signals. NY-MFA provides in **c** resolution bounds for $s = 4$ and $s = 5$ in excess of Gabor–Heisenberg limit $1/\pi$

$$[\Delta\tau\Delta B]_{\mathrm{NY-MFA}} = 1/s, \tag{6}$$

where $s = 2, 3, 4, 5$.

Here $\Delta\tau$ and ΔB, as given by (6), are not transforms of each other in the usual sense. However, $\Delta\tau$ and ΔB are the *only observed* widths.

The *true* NY-MFA amplitude sub-spectrum is extracted from Fourier transformation of multi-resolution signals. As shown in appendix B, thresholding works for such extraction. The signal in the time domain is reconstructed by applying inverse Fourier transformation. A natural extrapolation is obtained (see Sect. 1).

3.2 The lattice transform

Time and frequency resolutions of STFT resolution limits ($T\Delta B = 1$) are represented by the outer square. According to (6), decreasing lengths of analysis windows $\Delta\tau/T = \{1, 0.5, 0.33, 0.25, 0.2\}$ for, respectively, $s = 1, 2, 3, 4, 5$ do not degrade the *constant* frequency width ΔB that defines frequency resolution. Detrimental effects on frequency resolution of STFT for increasing time resolutions $\Delta\tau = T/s$ are therefore clearly eliminated. It is important to notice that since analysis window slides along the time axis with shorter and shorter lengths, without detrimental effects on frequency resolution, then the concept of frequency is more precisely approached making the assumption of stationarity attached to each local section more thoroughly justified when compared to STFT.

Now, let us consider the Gabor–Heisenberg inequality [12], i.e.,

$$[\sigma_\tau \sigma_B]_{\mathrm{G-H}} \geq 1/(4\pi), \tag{7}$$

where σ_τ and σ_f denote standard deviations, respectively, in the time and frequency domains.

For the sake of comparison, let us rewrite (7) for the widths ΔB and $\Delta\tau$ (roughly twice the standard deviations σ_τ and σ_B). This gives,

$$[\Delta\tau \Delta B]_{\mathrm{G-H}} \geq 1/\pi. \tag{8}$$

One notes that unlike the widths in the time and frequency domains of (6), here the widths, as given by (8), are transforms of each other in the usual sense. However, the two expressions (6) and (8) use *only observed* widths in the time and frequency domains. Now, based on this fact, it can be seen that the limit $1/s$, as given by (6), is in excess of Gabor–Heisenberg limit, $1/\pi$, in (8) for $s = 4$ and $s = 5$. This represents the novelty at the heart of NY-MFA.

3.3 Computation times

As pointed out in [24], one of the important advantages of NY-MFA is its easier implementation since the popular, elegant and efficient FFT algorithm remains used for all computations. A comparison of interest concerns computation times of standard Fourier transform (FT) and NY-MFA denoted, respectively, τ_{FT} and τ_{MFA} as a function of the resolution level. Let us recall that if N represents the length of the observed signal, then the length of a multi-resolution signal constructed from the only observed one is $2sN$ where $s = 2, 3, 4, 5$ is the resolution level. It is well known that FFT algorithm requires a number of calculations proportional to $N \log N$ where N is a power of 2.

3.3.1 Even resolution levels

If N is a power of two, then $2sN$ can be a power of two only for even resolution levels $s = 2, 4$. Let us compute the ratio $\tau_{\mathrm{MFA}}/\tau_{\mathrm{FT}}$ for an FFT algorithm in this case. This gives,

$$\frac{\tau_{\mathrm{MFA}}}{\tau_{\mathrm{FT}}} = \frac{2s \log 2sN}{\log N}. \tag{9}$$

One finds immediately that in most applications $N \gg 2s$. This therefore yields,

$$\forall\, s = 2, 4, \qquad \frac{\tau_{\mathrm{MFA}}}{\tau_{\mathrm{FT}}} \simeq 2s. \tag{10}$$

As shown by (10), ratio of computation times increases proportionally to *even* resolution levels, $s = 2, 4$.

3.3.2 Odd resolution levels

If N is a power of two, then for odd resolution levels $s = 3, 5$, the number of points $2sN + \delta N(s)$ becomes a power of two, where $\delta N(s)$ is the additional zero padding. One finds immediately that,

$$\delta N(s) = 2N(s-2). \tag{11}$$

This means that additional zeros padding for which $2sN + \delta N(s)$ becomes a power of two is always given by (11) for odd resolution levels. This gives,

$$\frac{\tau_{\mathrm{MFA}}}{\tau_{\mathrm{FT}}} = \frac{4(s-1))\log 4N(s-1)}{\log N}. \tag{12}$$

Since in most applications $N \gg 4(s-1)$, (12) yields,

$$\forall\, s = 3, 5, \qquad \frac{\tau_{\mathrm{MFA}}}{\tau_{\mathrm{FT}}} \simeq 4(s-1). \tag{13}$$

Here also, ratio of computation times increases proportionally to resolution levels.

3.3.3 Conclusion

By combining (10) and (13), ratio of computation times increases proportionally to resolution levels, $s = 2, 3, 4, 5$. One finds that computation times for $s = 3$ and $s = 4$ are identical. One therefore chooses the level $s = 4$ for its highest resolution.

4 NY-MFA of time-varying spectra

For a $T-$duration signal characterized by a time-varying amplitude spectrum, we first multiply this signal by a window defined to be nonzero over a short period of time $\Delta\tau = T/s$ ($s = 2, 3, 4, 5$), and secondly, we apply NY-MFA by following the 3 steps procedure:

1. We use the sub-signal of length $\Delta\tau$ to construct multi-resolution signals whose length is $2s\Delta\tau$ in accordance with (3) as a function of the desired resolution level $s = 2, 3, 4, 5$.
2. Fourier transformation of constructed multi-resolution signal is taken. NY-MFA amplitude spectrum results.
3. NY-MFA *true* amplitude spectrum is extracted from the amplitude spectrum of step 2 by means of thresholding.

This procedure is repeated for each sub-signal as the window slides along the time axis. We assume that each local section is stationary. Assumption of stationarity is more thoroughly justified than STFT since shorter and shorter analysis lengths $\Delta\tau = T/s$ $(s = 2, 3, 4, 5)$ have no detrimental effects on frequency resolution. This means also that application of above NY-MFA results, as recalled in Sect. 2 for stationary signals, is straightforward. This is detailed hereafter for each sub-signal.

4.1 Signal decomposition

Consider a T-duration signal $x_T(t)$ with time-varying spectrum and a rectangular window $\Pi_{\Delta\tau}(t - k\Delta\tau)$ where $\Delta\tau$ is its width and $k\Delta\tau$ $(k = 0, \ldots, K-1)$ are instants denoting its positions on the time axis, i.e.,

$$\Pi_{\Delta\tau}(t - k\Delta\tau) = \begin{cases} 1, & k\Delta\tau \le t \le (k+1)\Delta\tau \\ 0, & \text{otherwise.} \end{cases} \tag{14}$$

Decomposition of $x_T(t)$ by means of the window (14) yields,

$$\begin{aligned} x_T(t) &= \sum_{k=0}^{K-1} x_T(t)\Pi_{\Delta\tau}(t - k\Delta\tau) \\ &= \sum_{k=0}^{K-1} x_{\Delta\tau}(t - k\Delta\tau). \end{aligned} \tag{15}$$

Here, the K sliding windows do not overlap. We have therefore K subintervals corresponding to K sub-signals (defined in K local sections) of constant length $\Delta\tau$.

4.2 Multi-resolution signals

Now, each kth original sub-signal $x_{\Delta\tau}(t-k\Delta\tau)$ is considered *stationary* in the time interval defined by the width $\Delta\tau$. Let us apply the "s-resolution" operator $\Re_{(s)}$ to the signal defined by (15). Since $\Re_{(s)}$, as defined by (3) is a linear operator, we can write,

$$\Re_{(s)}[x_T(t)] = \sum_{k=0}^{K-1} \Re_{(s)}[x_{\Delta\tau}(t - k\Delta\tau)]. \tag{16}$$

According to (3), application of the "s-resolution" operator to any $\Delta\tau-$duration signal $x_{\Delta\tau}(t - k\Delta\tau)$ provides a new signal denoted $\widehat{x}_{2s\Delta\tau}(t - k\Delta\tau)$. Notice that the length of its time interval, as shown by its lower script, is now $2s\Delta\tau$ where $s = 2, 3, 4, 5$. By using this result, we can write (16) under the form,

$$\Re_{(s)}[x_T(t)] = \sum_{k=0}^{K-1} \widehat{x}_{2s\Delta\tau}(t - k\Delta\tau). \tag{17}$$

Clearly, instants $k\Delta\tau$, denoting positions of the window on the time axis, are not affected by applied resolution. Resolution affects only the chosen length $\Delta\tau$ of the sub-signal $x_{\Delta\tau}(t - k\Delta\tau)$. The resulted signal $\widehat{x}_{2s\Delta\tau}(t - k\Delta\tau)$ is called here the kth multi-resolution sub-signal.

4.3 NY-MFA sub-spectrum

Immediate application of recalled results in Sect. 2 to these stationary sub-signals "cut-out" from $x_T(t)$ is straightforward. Hence, by using the result, as given by (4) (spectra are now indexed by the integer, k, and T is replaced by $\Delta\tau$), the kth multi-resolution sub-signal $\widehat{x}_{2s\Delta\tau}(t - k\Delta\tau)$ in the frequency domain is given by,

$$\begin{aligned} \mathrm{FT}\,[\widehat{x}_{2s\Delta\tau}(t - k\Delta\tau)] &= \widehat{X}_k(f, 1/(s\Delta\tau)) \\ &= X_k(f) \star H_k(f, 1/(s\Delta\tau)), \end{aligned} \tag{18}$$

where FT$[x]$ represents the Fourier transform of x and $\widehat{X}_k(f, 1/(s\Delta\tau))$ represents the amplitude spectrum of $\widehat{x}_{2s\Delta\tau}(t - k\Delta\tau)$ whose spectral components are separated by the mutual distance $1/(s\Delta\tau)$. Here $X_k(f)$ is kth *true sub-spectrum* of the *original stationary* sub-signal from which $x_{\Delta\tau}(t-k\Delta\tau)$ is "cut-out." We assume that $X_k(f)$ is bandlimited. Here, $H_k(f, 1/(s\Delta\tau))$ is the transform of the resulted window starting at the instant $k\Delta\tau$. The main lobe width between its 3-dB levels is $1/(s\Delta\tau)$.

4.4 NY-MFA true amplitude spectrum

According to demonstration scheme of appendix B, the amplitude spectrum, as given by (50), can be rewritten here for the kth multi-resolution stationary signal. This gives,

$$\begin{aligned} \widehat{X}_k(f, 1/(s\Delta\tau)) &= X_k(f) \star H_k(f, 1/(s\Delta\tau)) \\ &= X_{\Pi_k}(f, 1/(s\Delta\tau)) + X_{\xi_k}(f, 1/(s\Delta\tau)), \end{aligned} \tag{19}$$

As shown in appendix B, spectral lines of $X_{\Pi_k}(f, 1/(s\Delta\tau))$ are much more powerful than those of $X_{\xi_k}(f, 1/(s\Delta\tau))$. For extraction of the true amplitude spectrum $X_{\Pi_k}(f, 1/(s\Delta\tau))$, convenient filtering able to preserve the first right-hand side of (19) and discard its second right-hand side is thresholding (hard or soft). In Sect. 5, examples of extraction of true amplitude spectra by means of thresholding are proposed.

Now, generalization of above results as given by (19) to all sub-spectra for $k = 0, \ldots, K-1$ is straightforward, and one obtains by summing up all these sub-spectra NY-

MFA resolved time-varying amplitude spectrum of the signal $x_T(t)$.

4.5 Computation times

Since the observed signal $x_T(t)$ with time-varying spectrum is divided into K non-overlapping local sections, then ratio of total computation times for, respectively, Fourier transform (FT) and NY-MFA is given by,

$$\frac{\sum_{k=0}^{K-1}\tau_{\mathrm{MFA}}^{(k)}}{\sum_{k=0}^{K-1}\tau_{\mathrm{FT}}^{(k)}}=\frac{\tau_{\mathrm{MFA}}}{\tau_{\mathrm{FT}}}=\begin{cases}2s, & s=2,4\\ 4(s-1), & s=3,5.\end{cases} \tag{20}$$

Ratio of computation times is independent of the number of local sections. Conclusion resulting from combination of (10) and (13) remain valid here.

5 Method and results

In this section, we observe that division of the time interval into smaller and smaller local sections does not degrade frequency resolution in accordance with (6). For computation of NY-MFA spectrum, we apply the 3 steps procedure described in Sect. 4. We show also that since analysis window slides along the time axis with shorter lengths, without detrimental effects on frequency resolution, then frequency is more precisely approached and its changes more precisely tracked.

5.1 Simulated signals

5.1.1 Definitions

Let us consider two *concatenated* sinusoids of respective normalized frequencies $f_1/f_e=0.1$ and $f_2/f_e=0.106$, where f_e is the sampling frequency. Observation intervals of the two sinusoids are identical and given by $N_1=N_2=256$ points. Here we have:

1. the *nominal* transition between the two sinusoids is obtained for $N_t=256$
2. the *nominal* frequency separation $\Delta\mathcal{B}/f_e=(f_2-f_1)/f_e=0.006$.

The corresponding number of points needed by STFT is $N=167$ since,

$$[N\Delta B/f_e]_{\mathrm{STFT}}=1. \tag{21}$$

The total observation interval of the two sinusoids, $N_T=N_1+N_2$, can only be divided into $R=3$ local sections.

Now, by rewriting NY-MFA uncertainty relation (6), we have,

$$[\mathcal{N}\Delta B(s)/f_e]_{\mathrm{NY-MFA}}=1/s, \tag{22}$$

where $\Delta B(s)/f_e$ is the normalized frequency separation dependent on the resolution, s ($s=2,3,4,5$), and $\mathcal{N}=\Delta\tau f_e$ is the number of points of each local section.

5.1.2 NY-MFA resolution properties

Let us divide the length of observation interval N_T into much smaller intervals and find how NY-MFA is able to resolve the above frequencies as a function of the desired resolution level. Let us choose, for example, to divide the observation interval into $K=12$ non-overlapping subintervals, each of which contains $\mathcal{N}=42$ points. By setting $\mathcal{N}=42$ and using (22), one finds the following frequency separations that NY-MFA is able to display for the resolutions $s=2,3,4,5$,

$$\begin{aligned}\Delta B(2)/f_e&=0.012\\ \Delta B(3)/f_e&=0.008\\ \Delta B(4)/f_e&=0.006\\ \Delta B(5)/f_e&=0.005.\end{aligned} \tag{23}$$

This means if one wants to find frequencies separated by the mutual *nominal* distance $\Delta\mathcal{B}/f_e=0.006$, one have to apply fourfold ($s=4$) or fivefold resolution ($s=5$); otherwise, one finds remaining frequency separations for $s=2$ or $s=3$. Conversely, if one wants to depict the nominal frequency separation $\Delta\mathcal{B}/f_e=0.006$ by using only double resolution ("$s=2$") because it is of simpler implementation and has reduced computation times, then by using (22), the chosen length of observation interval is given by $\mathcal{N}=84$ points. In this case, the total observation interval N_T is divided into $K=6$ non-overlapping subintervals. It can thus be seen that in all cases, the number of NY-MFA local sections K is greater than the number of local sections R of STFT for the same length of observed signal : $K>R$. This shows that assumption of stationarity attached to each local section of a signal is thoroughly justified by NY-MFA comparatively to STFT, and consequently, the concept of frequency is more precisely approached than wavelets and STFT can do. This demonstrates the ability of NY-MFA to track more precisely frequency changes as its analysis window slides along the time axis with shorter lengths without detrimental effects on frequency resolution.

5.1.3 STFT and wavelets

One can see in plots (a) and (b) of Fig. 2 two different views of the amplitude spectrum yielded by STFT for the division of the above observation interval ($K=12$ subintervals each of which contains $\mathcal{N}=42$ points). As expected, we have

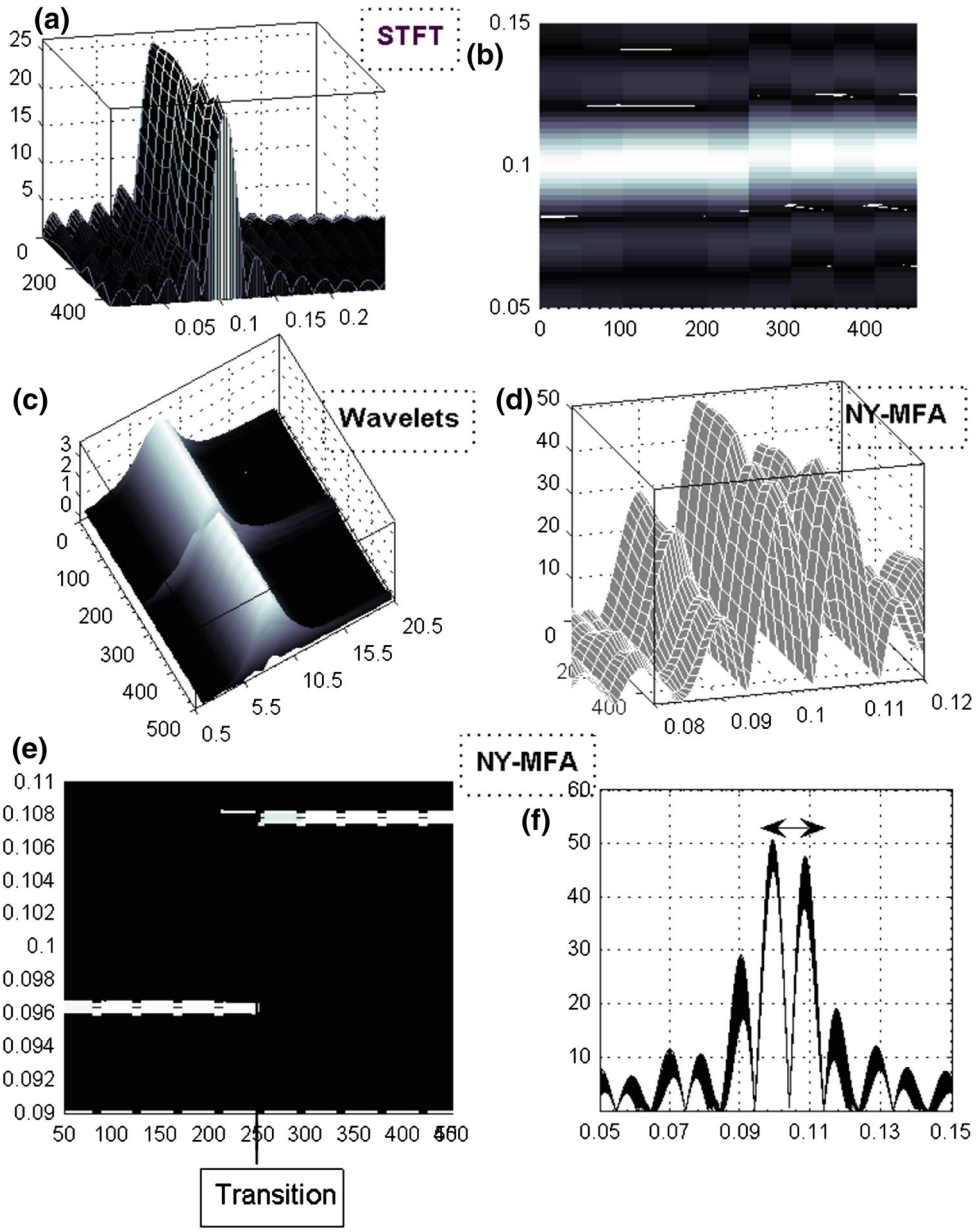

Fig. 2 Plots **a** and **b** represent two views of the STFT outcome. Wavelets analysis and NY-MFA twofold amplitude spectrum (without filtering) are depicted, respectively, in **c** and **d**. Two views of NY-MFA resolved frequencies are shown in **f** and **e**. Trade-off between time and frequency resolutions is clearly overcome

strongly blurred (widened) frequencies in (a) or (b), whereas transition that defines frequency changes is slightly detected in (b). Decreasing lengths of observation intervals have detrimental effects on frequency resolution. Wavelet analysis is shown by plot (c). Time and frequency resolution depends on the choice of the mother wavelet [32]. Here, we have chosen "morlet" wavelet since it is convenient for the signal under analysis (a priori information). We note that the instant at which frequency changes is depicted by plot (c) but frequencies, broadened by small observation intervals, are not resolved. This result remains unchanged when using other mother wavelets as those taken from the family of symlets (nearly symmetrical wavelets [21]). This is quite expected since wavelets are not suitable for restitution of precise frequency contents.

5.1.4 Twofold NY-MFA amplitude spectrum

The 3-steps procedure for computation of NY-MFA amplitude spectrum, as described in Sect. 4, is followed here. Let us use the double resolution (simpler implementation and reduced computation times). By setting $s = 2$, (3) and (19) yield for any sub-signal of length $\Delta\tau$ indexed by the integer $k = 0, \ldots, K-1$ its double resolution signal and corresponding twofold amplitude spectrum, i.e.,

$$\Re_{(2)}[x_{\Delta\tau}(t-k\Delta\tau)] = \Pi_{4\Delta\tau}(t-k\Delta\tau)\sum_{p=0}^{1} x_{\Delta\tau}(t-k\Delta\tau-2p\Delta\tau)$$

$$\mathrm{FT}[\Re_{(2)}[x_{\Delta\tau}(t-k\Delta\tau)] = X_{\Pi_k}(f,1/(2\Delta\tau)) + X_{\xi_k}(f,1/(2\Delta\tau)), \quad (24)$$

where FT[x] is the Fourier transform of x, and $\Pi_{4\Delta\tau}(t)$ is the rectangular window of length $4\Delta\tau$.

Hence, we expect normalized frequency separation given by $\Delta B(2)/f_e = 0.012$ since the length of each local section is $\mathcal{N} = 42$ points and $K = 12$ represents the total number of non-overlapping local sections. Frequencies are therefore localized with a precision dependent on the double resolution ($s = 2$). NY-MFA twofold amplitude spectrum defined for $s = 2$, as given by (24), is depicted by the plot (d) (without any thresholding). In plot (f), which is an other view of plot (d), one can see that our frequencies are clearly discriminated. After thresholding the spectrum of plot (d), plot (e) shows the *true* spectrum $X_{\Pi_k}(f,1/(2\Delta\tau))$, as given by the first right-hand side of (24). Let us note that thresholding used here preserves only powerful lines and discards weaker ones. Transition at which frequency changes is visible and occurs for the point $N_t = 255$. Frequency leakage decreases and lines gather at the vicinity of true frequencies. One can read from plot (e) two clear normalized frequency lines located, respectively, at $\widehat{f_1}/f_e = 0.096$ and $\widehat{f_1}/f_e = 0.108$, which corresponds to $(\widehat{f_2} - \widehat{f_1})/f_e = 0.012$. Precisions with which nominal frequencies are depicted are, respectively, 4 and 2 %. Spectra in (a), (c) and (e) of, respectively, STFT, Wavelts and NY-MFA show that usual trade-off between the length of observation intervals and frequency resolutions is clearly overcome by NY-MFA. It can thus be seen that one combines easily decreasing lengths of analysis windows without deteriorating frequency resolution by means of NY-MFA.

5.2 Doppler velocimetry

5.2.1 Introduction

It is well known that Doppler spectrum analysis provides non-invasive means to measure flow velocities. In clinical applications, Doppler signals are frequently used for various diagnoses as arterial occlusive disease or atherosclerosis [30–32]. Time-frequency mapping of the Doppler blood flow signal represents time-varying velocity of blood flow [32]. Traditionally, STFT is used to analyze such time-varying velocity. It is reported in [32] that fixed length of the time-frequency analysis window of STFT introduces inaccuracies for analysis of velocities that change rapidly with time. Comparatively to STFT, wavelet transforms have flexible time-frequency windows and therefore capture more efficiently velocities having relatively wide bandwidths. Since wavelet transforms (WT) generate a time-frequency representation with better resolution, WT are used as an alternative signal processing tool to the STFT for Doppler blood flow signals [31,32] in spite of the fact that:

1. Resolution is dependent on the choice of the mother wavelet.
2. Wavelets are not suitable for precise frequency or velocity tracking.

5.2.2 Definitions

We have a Doppler signal whose duration is $T = 34.4 \times 10^{-3}$ s. The used sampling frequency is $f_e = 120$ kHz. The total number of points of the record is $N_T = 4128$ points. Let us assume that desired frequency tracking is based on detection of the normalized frequency separation $\Delta\mathcal{B}/f_e = 1.66 \times 10^{-3}$ or equivalently $\Delta\mathcal{B} = 200$ Hz. The corresponding length of observation interval for STFT, as given by (21), is $N = 602$. This means that the observation interval N_T can only divided into only $R = 6$ sections if STFT is used.

Now, by using (22), the length of the sliding window is $\mathcal{N} = 120$ points (or 10^{-3}s), for NY-MFA fivefold resolution ($s = 5$). The observation interval N_T can be divided into $K = 34$ sections. NY-MFA combines therefore short time window, 10^{-3}s, able to track frequency changes up to the resolution 200 Hz over $K = 34$ local sections. Here also one notes that since $K \gg R$, the frequency (velocity) together with its changes, are more precisely approached and tracked for such a fine division of the observation interval.

5.2.3 NY-MFA of Doppler signals

The 3-steps procedure for computation of NY-MFA amplitude spectrum (Sect. 4) is followed here. By setting $s = 5$, (3) and (19) yield for any sub-signal of length $\Delta\tau$ indexed by the integer $k = 0, \ldots, K-1$ its fivefold resolution signal and corresponding Fourier transform, i.e.,

$$\Re_{(5)}[x_{\Delta\tau}(t-k\Delta\tau)] = \Pi_{10\Delta\tau}(t-k\Delta\tau)\sum_{p=0}^{1}[x_{\Delta\tau}(t-k\Delta\tau-5p\Delta\tau) + x_{\Delta\tau}((5p+2)\Delta\tau-(t-k\Delta\tau))]$$

$$\mathrm{FT}[\Re_{(5)}[x_{\Delta\tau}(t-k\Delta\tau)] = X_{\Pi_k}(f,1/(5\Delta\tau)) + X_{\xi_k}(f,1/(5\Delta\tau)), \quad (25)$$

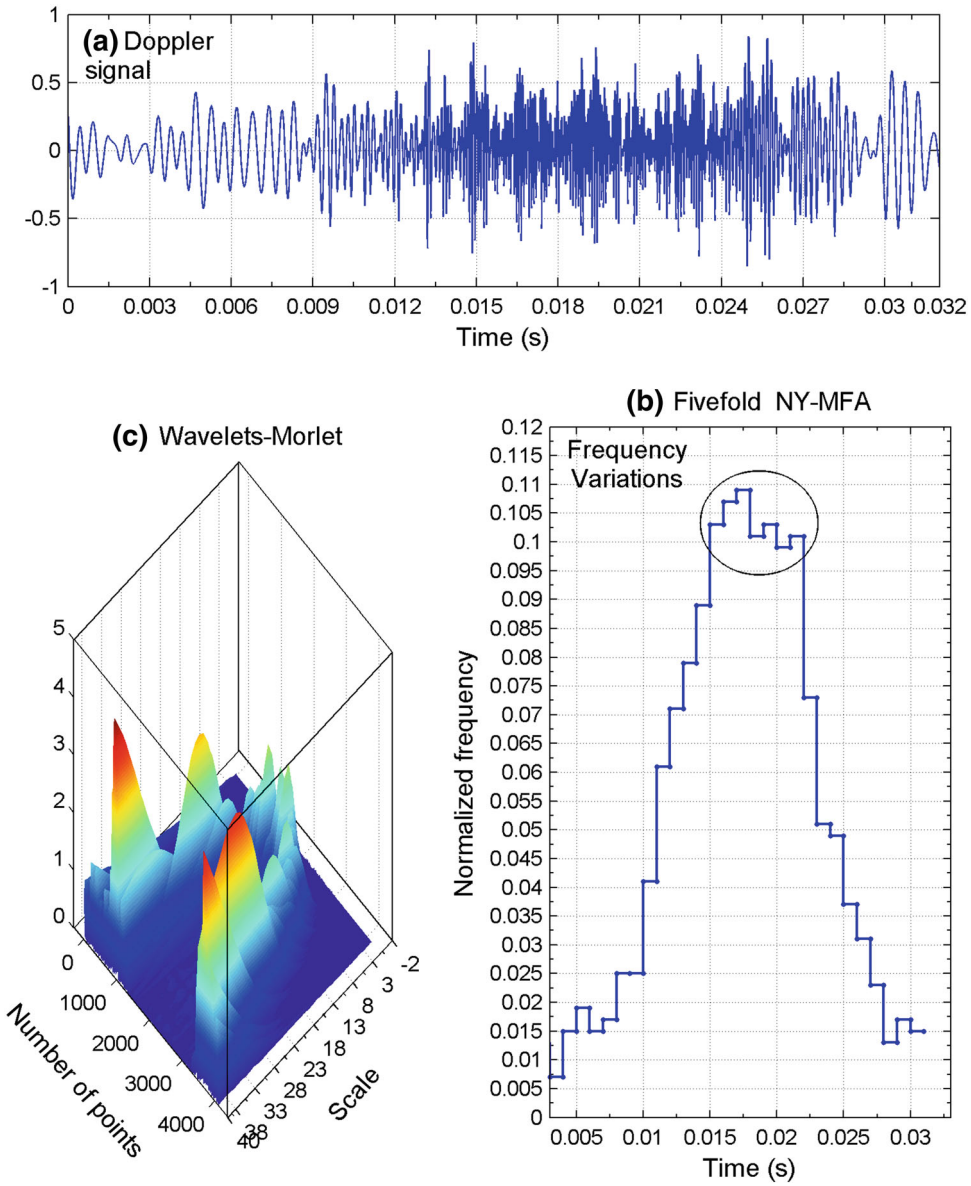

Fig. 3 Frequency or velocity tracking. NY-MFA fivefold frequency variations in **b** of the non-stationary Doppler signal in **a** tracks frequency changes of 200 Hz over 10^{-3} s. The *circle* in **b** indicates the interval [0.015, 0.022](s) where maxima of frequency variations are detected. Frequency spreading of wavelet analysis in **c** prevents detection of such frequency changes

where FT[x] is the Fourier transform of x and $\Pi_{10\Delta\tau}(t)$ is the rectangular window of length $10\Delta\tau$.

Results are summarized in Fig. 3. Here, we have chosen NY-MFA fivefold amplitude spectrum for its precise frequency (velocity) tracking. Plot 3(a) shows Doppler signal in the time domain. Frequency variations of NY-MFA fivefold resolved spectrum are depicted in plot 3(b) over $K = 34$ local sections where the circle indicates the interval in which maxima of frequency variations are detected. Here also thresholding preserves only powerful lines and discards weaker ones. Now, for the sake of comparison and checking provided results, Fig. 4 shows detailed views in the time domain through plots 4(a)–(d) of the analyzed Doppler signal in 3(a). One finds that:

- plot 4(a) depicts in [0, 0.015] (s) increased frequency variations,
- frequency variations achieve the highest values in plot 4(b) defined for [0.015, 0.022](s).
  This interval is indicated by a circle in plot 3(b),
- plot 4(c) shows in [0.022, 0.026] a frequency decreasing effect that continues on in plot 4(d) or in [0.026, 0.034](s).

One can see visually that NY-MFA frequency variations in 3(b) are in accordance with detailed views of Fig. 4 in the time domain. Observation results of NY-MFA, as shown in Figs. 3 and 4, track fast velocity changes in time and provide time-

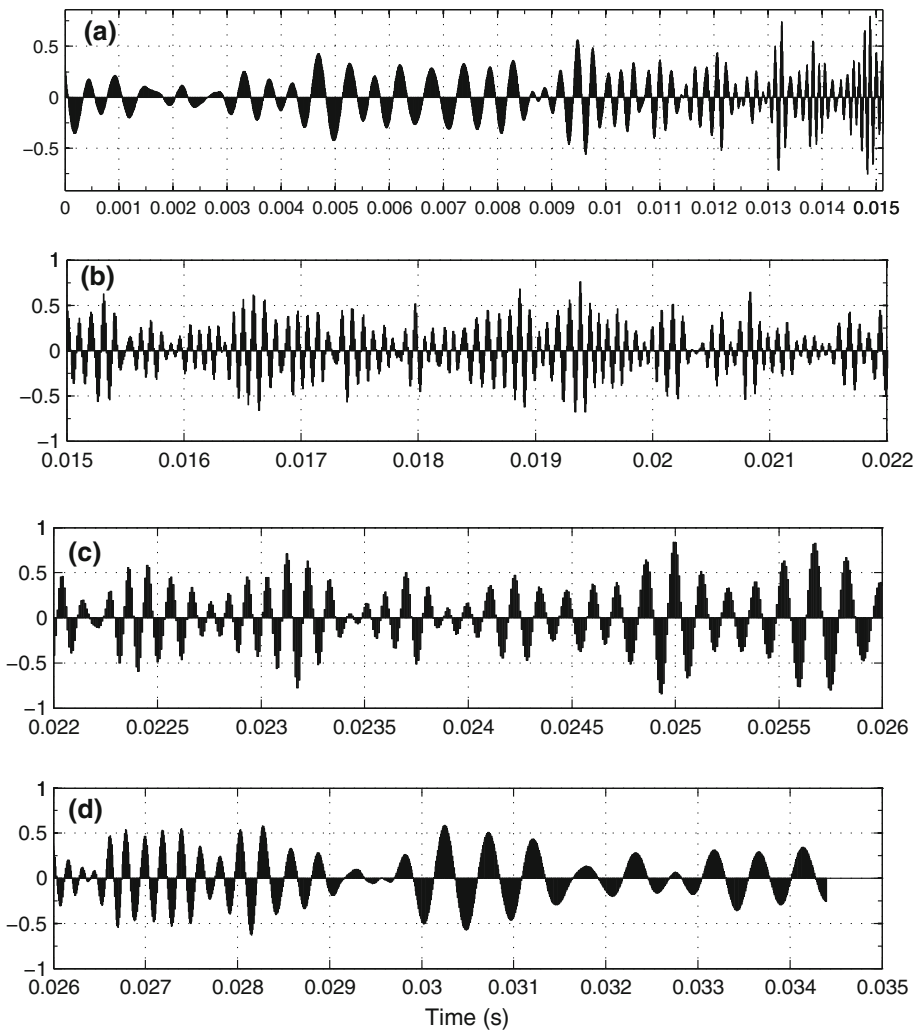

Fig. 4 Detailed views in the time domain of the Doppler signal of Fig. 3a compared with detected NY-MFA frequency variations in Fig. 3b

frequency representations with satisfactory time-frequency resolutions in accordance with (6).

5.2.4 Wavelets

Wavelet analysis by means of the mother wavelet morlet, more suitable for this signal, is shown in plot 3(c) for comparison. It can be seen that important frequency spreading cannot discriminate frequency changes up to 200 Hz. Clearly, frequency spreading results from reduction in the size of analysis windows. Hence, no comparable and precise velocity changes in the time-frequency plane are depicted.

6 Conclusion

Multi-resolution analysis framework, labeled NY-MFA, suitable for signals with time-varying spectra is proposed in this work. Provided lattice transform in the time-frequency plane uses only observed signals to eliminate classical trade-off of time-frequency or timescale representations with resolution bounds in excess of Gabor–Heisenberg limit. High time resolution is combined with suppression of strong frequency blurring. We have shown that since analysis window of NY-MFA slides along the time axis with shorter and shorter lengths, without detrimental effects on frequency resolution, assumption of stationarity attached to each local section is more thoroughly justified, and consequently, the frequency with its changes is more precisely approached and tracked than wavelets and short-term Fourier transform can do. Observation results with their increased time resolutions, discriminated and precise frequency contents are in accordance with theoretical predictions.

Acknowledgments The author would like to thank anonymous reviewers for their pertinent questions, helpful comments and valuable discussions.

7 Appendix A

Here, we use the only observed stationary signal $x_T(t)$ in the time interval of length T to construct a double resolu-

tion signal for which $T\Delta B = 1/2$ is satisfied. We propose "one-point" interpolation followed by zeros insertion in the frequency domain [24]. Notice that we propose here a simpler formulation of original computations appearing in [24].

7.1 One-point interpolation

Given $x_T(t)$, let us construct the *overall* signal defined in $[0, 2T]$ as follows,

$$\widehat{x}_{2T}(t) = \Pi_{2T}(t)[x_T(t) + z_T(t-T)], \tag{26}$$

where $z_T(t) = 0, \forall t \in [0, T]$ and $\Pi_{2T}(t)$ is the rectangular window of length $2T$. By writing $\widehat{x}_{2T}(t)$ as a function of the true signal $x_{2T}(t)$, we obtain,

$$\widehat{x}_{2T}(t) = \Pi_{2T}(t)x_{2T}(t)\Pi_T(t). \tag{27}$$

One can see easily that (27) can be put under the form,

$$\widehat{x}_{2T}(t) = x_{2T}(t) \times w_{2T}(t), \tag{28}$$

where the window $w_{2T}(t)$ is given by,

$$w_{2T}(t) = [\Pi_{2T}(t) + \xi_{2T}(t)]/2, \tag{29}$$

and $\xi_{2T}(t) = \Pi_T(t) - \Pi_T(t-T)$.

7.2 Zeros insertion in the frequency domain

In order to insert zeros on the frequency axis able to define the *bounded support*, $1/(2T)$, we introduce a *local period* by substituting $4T$ for $2T$ in the subscripts of (28). This gives,

$$\widehat{x}_{4T}(t) = w_{4T}(t) \sum_{p=0}^{1} x_{2T}(t-2pT). \tag{30}$$

It is easy to see that $w_{4T}(t)$ has the following Fourier transform,

$$W_4(f) = (H_{\Pi_4}(f) + H_{\xi_4}(f))/2, \tag{31}$$

where $H_{\Pi_4}(f)$ and $H_{\xi_4}(f)$ are, respectively, Fourier transforms of $\Pi_{4T}(t)$ and $\xi_{4T}(t)$, i.e.,

$$\begin{aligned} H_{\Pi_4}(f) &= 4T\phi_{\Pi_4}(f)\, S(4\pi fT), \\ H_{\xi_4}(f) &= -\imath 4T\, S(\pi fT)\sin(\pi fT)\cos(2\pi fT), \end{aligned} \tag{32}$$

where $S(x) = \sin(x)/x$. The complex exponential $\phi_{\Pi_4}(f)$ represents phase induced by the absolute position of the time interval on the timescale. Notice that,

$$\forall\, f, \quad |H_{\Pi_4}(f)| > |H_{\xi_4}(f)|. \tag{33}$$

7.3 Bandwidth

Here, our aim is to derive the bandwidth of $W_4(f)$ as given by (31). Notice that $W_4(f)$ consists of two terms. Let us consider the first term $H_{\Pi_4}(f)$. One can see from (32) that the interval for which $S(4\pi fT) = 0$ for $f = k/(4T)$ where $k \pm 1$ is given by $1/(2T)$. Now, the bandwidth, defined as the main lobe width between 3-dB or $1/\sqrt{2}$ of $H_{\Pi_4}(f)$, is so that,

$$\mathrm{Bw}\left[H_{\Pi_4}(f)\right] = 1/(4T). \tag{34}$$

On the other hand,

$$\begin{aligned} &H_{\Pi_4}(f)\big|_{f=\pm 1/(4T)} \\ &= H_{\xi_4}(f)\big|_{f=\pm 1/(4T)} = H_{\xi_4}(f)\big|_{f=0} = 0, \end{aligned} \tag{35}$$

and particularly for points defining the bandwidth of $H_{\Pi_4}(f)$, we have,

$$|H_{\xi_4}(f)|\big|_{f=1/(8T)} \ll |H_{\Pi_4}(f)|\big|_{f=1/(8T)}. \tag{36}$$

The bandwidth remains unchanged by the additional term $H_{\xi_4}(f)$. It follows from (34) and (36) that the bandwidth of $W_4(f)$, as given by (31), is so that,

$$\mathrm{Bw}\,[W_4(f)] \simeq \mathrm{Bw}\left[H_{\Pi_4}(f)\right] = 1/(4T). \tag{37}$$

7.4 Double resolution properties

By considering (30) in the frequency domain, we can write,

$$\begin{aligned} \mathrm{FT}[\widehat{x}_{4T}(t)] &= \mathrm{FT}\left[\sum_{p=0}^{1} x_{2T}(t-2pT)\right] \star W_4(f), \\ &= X(f) \star \theta(2fT) H_{\Pi_2}(f) \star W_4(f), \end{aligned} \tag{38}$$

where $\mathrm{FT}[x]$ is the Fourier transform of x. Here $X(f)$ and $H_{\Pi_2}(f)$ are, respectively, Fourier transforms of the signal $x(t)$ and the rectangular window $\Pi_{2T}(t)$ of length $2T$. Notice that $X(f)$, *the true amplitude spectrum*, is assumed bandlimited. Here the term $\theta(2fT)$ resulting from time translations is given by,

$$\theta(2fT) = \left[1 + e^{-\imath 2\pi(2fT)}\right]. \tag{39}$$

Notice that $\theta(2fT)$, as given by (39), defines the amplitude spectrum at the frequency locations $f = k/(4T)$. We have,

$$\begin{aligned} \forall\, f = k/(4T), \quad \theta(2fT) &= (1 + (-1)^k) \\ &= \begin{cases} 2, & k = 2p \\ 0, & k = 2p+1, \end{cases} \end{aligned} \tag{40}$$

where $p = 0, \pm 1, \pm 2 \ldots$.

Now, convolution between the windows $H_{\Pi_2}(f)$ and $W_4(f)$ whose bandwidths are, respectively, given by $1/(2T)$ and $1/(4T)$ yields a window with the broadest of the two bandwidths. According to (37), this gives

$$\begin{aligned} H(f, 1/(2T)) &= \theta(2fT) H_{\Pi_2}(f) \star W_4(f) \\ &= \begin{cases} 2(H_{\Pi_2}(f) \star W_4(f)), & k = 2p \\ 0, & k = 2p+1, \end{cases} \end{aligned} \tag{41}$$

where the bandwidth of $H(f, 1/(2T))$ is specified by its second argument $1/(2T)$.
By setting (41), (38) yields,

$$\begin{aligned}\mathrm{FT}[\widehat{x}_{4T}(t)] &= X(f) \star H(f, 1/(2T)) \\ &= \widehat{X}(f, 1/(2T)).\end{aligned} \tag{42}$$

As shown by (42), the true spectrum $X(f)$ is convolved with the filter $H(f, 1/(2T))$ whose bandwidth is $1/(2T)$. This yields the twofold resolution spectrum $\widehat{X}(f)$ for which,

$$T\Delta B = 1/2,$$

where T and ΔB are *widths* in time and frequency domains.

Extraction of the twofold amplitude spectrum $X(f, 1/(2T))$ of the signal is detailed in appendix B.

7.5 Expression of double resolution signals

By considering (30), the double resolution signal is given by,

$$\widehat{x}_{4T}(t) = w_{4T}(t) \sum_{p=0}^{1} x_{2T}(t - 2pT). \tag{43}$$

Here (43) can be written as a function of $x_T(t)$ as follows,

$$\widehat{x}_{4T}(t) = \Pi_{4T}(t) \sum_{p=0}^{1} x_T(t - 2pT), \tag{44}$$

which is given by $\Re_{(s)}[x_T(t)]$ for $s = 2$. Derivation of remaining multi-resolution signals for $s = 3, 4, 5$ is detailed in [24].

8 Appendix B

8.1 General case

Here, we extract the amplitude spectrum $X(f)$ of the signal $x(t)$ up to the resolution $1/(sT)$. We start by generalizing (42) to any level of resolution. This gives,

$$\begin{aligned}\mathrm{FT}[\Re_{(s)}[x_T(t)]] &= \widehat{X}(f, 1/(sT)) \\ &= X(f) \star H(f, 1/(sT)),\end{aligned} \tag{45}$$

where,

$$H(f, 1/(sT)) = \theta(sfT) H_{\Pi_s}(f) \star W_{2s}(f), \tag{46}$$

and $W_{2s}(f)$ is given by,

$$W_{2s}(f) = (H_{\Pi_{2s}}(f) + H_{\xi_{2s}}(f))/2. \tag{47}$$

By setting (47), (45) yields the two terms,

$$\begin{aligned}\widehat{X}(f, 1/(sT)) = {} & X(f) \star \theta(sfT) H_{\Pi_s}(f) \star H_{\Pi_{2s}}(f)/2 \\ & + X(f) \star \theta(sfT) H_{\Pi_s}(f) \star H_{\xi_{2s}}(f)/2\end{aligned} \tag{48}$$

For the sake of simplicity, let

$$\begin{aligned}X_\Pi(f, 1/(sT)) &= X(f) \star \theta(sfT) H_{\Pi_s}(f) \star H_{\Pi_{2s}}(f)/2 \\ X_\xi(f, 1/(sT)) &= X(f) \star \theta(sfT) H_{\Pi_s}(f) \star H_{\xi_{2s}}(f)/2.\end{aligned} \tag{49}$$

By using (49), we can rewrite (48) under the form,

$$\widehat{X}(f, 1/(sT)) = X_\Pi(f, 1/(sT)) + X_\xi(f, 1/(sT)), \tag{50}$$

Our aim, now, is to extract the spectrum $X(f)$ of the signal up to the resolution $1/(sT)$.

8.2 The spectrum of the signal

According to (49), $X(f)$ is involved in the expressions of $X_\Pi(f, 1/(sT))$ and $X_\xi(f, 1/(sT))$. Generalization of the important relation given by (33) to any level of resolution "s" yields,

$$\forall\, f, \quad |H_{\Pi_{2s}}(f)| > |H_{\xi_{2s}}(f)|. \tag{51}$$

Here (51) helps to find the convenient filtering able to extract $X(f)$ up to the resolution $1/(sT)$. Clearly, inequality (51) shows that spectral lines of $X_\Pi(f, 1/(sT))$ are much more powerful than those of $X_\xi(f, 1/(sT))$. Hence, the second right-hand side of (50) can be discarded and the first right-hand side preserved. Convenient filtering is therefore thresholding. We have shown in [25,26] that thresholding (hard or soft) applied to simulated and experimental signals works for extraction of the amplitude spectrum of the signal. This is also observed in this work.

8.3 Frequency resolution

Consider the first right-hand side of (50). Convolution between transforms $H_{\Pi_s}(f)$ and $H_{\Pi_{2s}}(f)$ yields a transform with the broadest $1/(sT)$ of the two bandwidths. This gives,

$$X_\Pi(f, 1/(sT)) = X(f) \star \theta(sfT) H_{\Pi_s}(f)/2. \tag{52}$$

Since $\forall\, f = k/(2sT)$, we have,

$$\theta(sfT) = \begin{cases} 2, & k = 2p \\ 0, & k = 2p + 1, \end{cases} \tag{53}$$

where $p = 0, \pm 1, \pm 2, \ldots$, then,

$$X_\Pi(f, 1/(sT)) = \begin{cases} X(f) \star H_{\Pi_s}(f), & k = 2p \\ 0, & k = 2p + 1. \end{cases} \tag{54}$$

One can see immediately that since $H_{\Pi_s}(f)$ is the transform of the rectangular window $\Pi_{sT}(t)$, the true amplitude spectrum of the signal defined for the resolution $1/(sT)$ is represented by (54), i.e.,

$$\forall\, f = k/(2sT) \text{ and } k = 2p,$$
$$X_{\Pi}(f, 1/(sT)) = X(f) \star H_{\Pi_s}(f)$$
$$= X(f, 1/(sT)), \tag{55}$$

where $p = 0, \pm 1, \pm 2 \ldots$.

References

1. Grochenig, K.: Foundations of Time-Frequency Analysis. Birkhauser, Boston, MA (2001)
2. Portnoff, M.: Time-frequency representation of digital signals and systems based on short-time Fourier analysis. IEEE Trans. Acoust. Speech Signal Process. **28**(1), 55–69 (1980)
3. Jones, D.L., Parks, T.W.: A resolution comparison of several time-frequency representations. In: International Conference on Acoustics, Speech, and Signal Processing, vol. 4, pp. 2222–2225. ICASSP-8, 23–26 May, 1989
4. Cohen, L.: Time-Frequency Analysis. Prentice-Hall, Englewood Cliffs, NJ (1995)
5. Nawab, S., Quatieri, T., Lim, J.: Signal reconstruction from short-time Fourier transform magnitude. IEEE Trans. Acoust. Speech Signal Process. **31**(4), 986–998 (1983)
6. Portnoff, M.: Short-time Fourier analysis of sampled speech. IEEE Trans. Acoust. Speech Signal Process. **29**(3), 364–373 (1981)
7. Portnoff, M.: Implementation of the digital phase vocoder using the fast Fourier transform. IEEE Trans. Acoust. Speech Signal Process. **24**(3), 243–248 (1976)
8. Qian, S., Chen, D.: Joint time-frequency analysis. IEEE Signal Process. Mag. **16**(2), 52–67 (1999)
9. Hlawatsch, F., Boudreaux-Bartels, G.F.: Linear and quadratic time-frequency signal representations. IEEE Signal Process. Mag. **9**, 21—67 (1992)
10. Almeida, L.B.: The fractional Fourier transform and time-frequency representations. IEEE Trans. Signal Process. **42**(11), 3084–3091 (1994)
11. Priestley, M.B.: Non-linear and Non-stationary Time Series Analysis. Academic Press, London (1988)
12. Gabor, D.: Theory of communication. J. Inst. Electron. Eng. **93**(11), 429–457 (1946)
13. Cohen, L.: Generalized phase space distribution functions. J. Math. Phys. **7**(5), 781–786 (1966)
14. Wigner, E.P.: On the quantum correction for thermodynamic equilibrium. Phys. Rev. **40**, 749–759 (1932)
15. Claasen, T.A.C.M., Mecklenbräuker, W.F.G.: The Wigner distribution, a tool for time-frequency analysis, Part I: continuous-time signals. Philips J. Res. **35**(3), 217–250 (1980)
16. Goupillaud, P., Grossman, A., Morlet, J.: Cycle-octave and related transforms in seismic signal analysis. Geoexploration **23**, 58–102 (1984)
17. Daubechies, I.: The wavelet transform, time-frequency localization and signal analysis. IEEE Trans. Inf. Theory **36**, 961–1005 (1990)
18. Auger, F., Flandrin, P.: Improving readability of time-frequency and time-scale representations by the reassignment method. IEEE Trans. Signal Process. **43**(5) (1995)
19. Meyer, Y.: Wavelets: algorithms and applications. Society for Industrial and Applied Mathematics, Philadelphia (1993)
20. Rioul, O., Vitterli, M.: Wavelets and Signal Processing. IEEE Signal Process. Mag. **8**(4), 14–38 (1991)
21. Daubechies, I.: Ten Lectures on Wavelets. SIAM, Philadaphia, PA (1992)
22. Daubechies, I.: The wavelet transform, time-frequency localization and signal analysis. IEEE Trans. Inf. Theory **36**(5), 961–1005 (1990)
23. Strang, G.: Wavelet transforms versus Fourier transforms. Bull. Amer. Math. Soc. **28**, 288–305 (1993)
24. Yahya Bey, N.: Multi-resolution Fourier analysis, Part I: fundamentals. Int. J. Commun. Netw. Syst. Sci. **4**(6), 364–371 (2011)
25. Yahya Bey, N.: Multi-resolution Fourier analysis, Part II: missing signal recovery and observation results. Int. J. Commun. Netw. Syst. Sci. **5**(1), 28–36 (2012)
26. Yahya Bey, N.: Multi-resolution Fourier analysis: extraction and missing signal recovery of short buried signals in noise. In: Signal Image and Video Processing (SIViP). Springer, Berlin (October 2012)
27. Calway, A.D., The Multiresolution Fourier Transform: A General Purpose Tool for Image Analysis. Ph.D Thesis, Warwick Univ. (1989)
28. Pearson, E.R.S.: The Multiresolution Fourier Transform and Its Application to the Analysis of Polyphonic Music. Ph.D. Thesis, Warwick Univ. (1991)
29. Wilson, R., Calway, A.D., Pearson, E.R.S.: A generalized wavelet transform for fourier analysis: the multiresolution fourier transform and its application to image and audio signals. IEEE Trans. Image Process. **38**, 674–690 (1992)
30. Sparto, P.J., Parnianpour, M.: Wavelet and short-time Fourier transform analysis of electromyography for detection of back muscle fatigue. IEEE Trans. Rehab. Eng. **8**(3), 433–436 (2000)
31. Gramatikov, B., Georgiev, I.: Wavelets as alternative to short-time Fourier transform in signal-averaged electrocardiography. Med. Biol. Eng. Comput. **33**(3), 482–487 (1995)
32. Zhang, Y., Guo, Z., Wang, W., He, S., Lee, T., Loew, M.: A comparison of the wavelet and short-time fourier transforms for Doppler spectral analysis. Med. Eng. Phys. **25**(7), 547–557 (2003)